A vector control strategy for five-phase drives fed by simplified split-source inverters

Dabour, Sherif; Aboushady, Ahmed; Elgenedy, Mohamed; Gowaid, Azmy; Farrag, M E A

Published in:
Proceedings of The 2023 IEEE Conference on Power Electronics and Renewable Energy

Publication date:
2023

Document Version
Author accepted manuscript

A Vector Control Strategy for Five-Phase Drives Fed by Simplified Split-Source Inverters

Sherif M. Dabour
Electrical Power and Machines Engineering Dept.
Tanta University
Tanta, Egypt
sherif.dabour@gcu.ac.uk

Ahmed A. Aboushady
Electrical and Electronics Engineering Dept.
Glasgow Caledonian University
Glasgow, UK
ahmed.aboushady@gcu.ac.uk

Mohamed. A. Elgenedy
Electrical and Electronics Engineering Dept.
Glasgow Caledonian University
Glasgow, UK
mohamed.elgenedy@gcu.ac.uk

I. A. Gowaid
Electrical and Electronics Engineering Dept.
Glasgow Caledonian University
Glasgow, UK
azmy.gowaid@gcu.ac.uk

Mohamed Emad Farrag
Electrical and Electronics Engineering Dept.
Glasgow Caledonian University
Glasgow, UK
mohamed.farrag@gcu.ac.uk

***Abstract*—Multiphase electric drives are required in several applications to provide high levels of reliability. A newly developed multiphase Simplified Split-Source Inverter (S^3I) provides a boost capability during sags in the input voltage. It also has a wider modulation range and a lower harmonic content than Z-Source Inverters. This paper proposes an Indirect Field-oriented Control (IFOC) strategy for a five-phase induction motor supplied by an S^3I. This control strategy can be divided into three parts. The first uses a dual control loop to control the dc-boosted voltage of the S^3I and regulate the input current. The second uses a conventional IFOC to control the motor speed and generate sinusoidal voltage references. With a newly developed space vector modulation approach, the third part will generate the switching pulses of the inverter switches. A series of simulations using PLECS and Python were conducted to verify the concept and illustrate the potential of the proposed drive system.**

Keywords— multiphase, vector control, split-source inverter, induction motor, space vector modulation

I. INTRODUCTION

There has been a recent trend in multiphase systems due to their increased reliability and reduced torque pulsations [1],[2]. These characteristics make them ideal candidates for critical applications, such as electric ship propulsion and locomotive traction [3]. The literature primarily focuses on five-phase induction motor-based systems because they have a good performance with a lower loss than the other architectures [4].

In principle, five-phase motors are powered by Voltage Source Inverters (VSIs) or Matrix Converters (MCs) and controlled in the same way as three-phase machines. Scalar control (i.e., V/f control) for open and closed loops does not attract much interest nowadays because they have sluggish responses. Consequently, field-oriented control, optimal current control, direct torque control, and predictive control are more relevant and widely applied to five-phase drives to obtain a good and more efficient performance [5]-[7].

Z-source Inverters (ZSIs) have been introduced as emerging topologies with interesting buck-boost characteristics [8]. As a result of these characteristics, ZSI-based drive systems become more reliable and desirable than those based on VSI [7], and MC [9], especially during supply voltage sags in electric vehicles. There is no doubt that ZSIs are no longer limited to single and three-phase systems but now extend to multiphase applications to improve their reliability [10]-[12].

An indirect FOC technique for a five-phase induction motor supplied by a bidirectional ZSI (BZSI) is introduced in [10]. Fig. 1 shows the power circuit topology of this system. Even though BZSI increases the reliability of multiphase drive systems, they control voltage gain within a narrow range by changing shoot-through duty ratios. Thus, any inaccuracy in ST duty cycle calculation results in a large difference in voltage gain. This will significantly impact the drive system's performance.

Recently, a Split-Source Inverter (SSI) was introduced as an alternative topology to ZSI. As a result, SSI finds its way into various topologies and applications. It can be configured in three ways: 1) a basic SSI that uses forward diodes to connect the boosting inductance to the midpoint of each inverter leg [13],[14], 2) a bidirectional split-source inverter, which replaces the forward diodes with bidirectional switches [15], and 3) a simplified split-source inverter (S^3I), which merges the topology of a buck-boost converter with the standard inverter circuit [16]. It is also used to obtain multilevel outputs [17]-[18] and in multiterminal converters [19],[20]. Quite recently, the split-source inverter has been extended to multiphase systems [21],[22]. It has potential advantages that can be summarized as follow:

- It provides boosted sinusoidal output waveforms with the continuous input current.
- It has a non-pulsed dc-link voltage.
- It uses only one inductor and a capacitor to obtain the boosting action.
- There is no need for ST control; therefore, it uses the same active and null vectors as the conventional VSI.

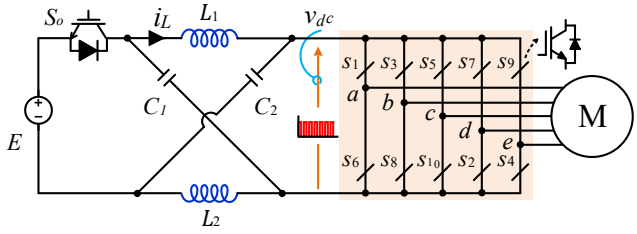

Fig. 1. Bidirectional ZSI-based five-phase IM drives [10].

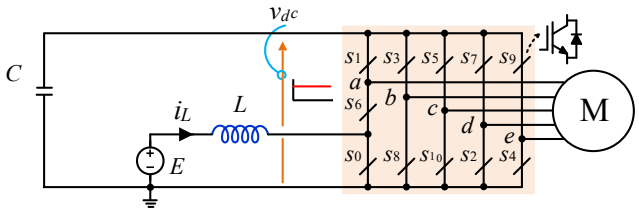

Fig. 2. Proposed S^{3}I-based five-phase IM drives.

This paper aims to replace the ZSI in the five-phase IM drive system shown in Fig. 1 with the S^{3}I to merge the merits of the SSI mentioned above with the five-phase system. The power circuit of the proposed system is shown in Fig. 2. As is evident from the diagram, the proposed topology consists of the same number of active switches as the BZSI. Despite this, fewer passive elements are used. Moreover, contrary to what happens in the ZSI, the input inductance and dc-link capacitance in S^{3}I of Fig. 2 maintain a continuous supply current and low ripple dc-link voltage. The paper also presents the IFOC for the proposed system. A new space vector modulation scheme and voltage decoupling compensation are used to implement the IFOC. Based on a small signal model of S^{3}I, a dual-loop controller is designed to regulate the peak dc-link voltage and the inductor current. PLECS simulations have validated the proposed IFOC speed control for five-phase IM.

II. Five-Phase S^{3}I

The power circuit of the proposed topology is shown in Fig. 2. In the following subsections, the operating modes and the modulation technique of the proposed topology are illustrated.

A. DC-boosting Operating-mode

As shown in Fig. 2, when the switch S_0 is closed, the supply current will flow though the inductor, which will store some energy while when the switch S_0 is opened, the energy stored in the inductor will be released. Taking a different perspective, the first leg of this topology (i.e., leg-a) has three switches (S_1, S_6, S_0). Only two of these switches must be connected at the same time to avoid any short-circuit on the capacitor or floating inductor's terminal. Moreover, the switching signals of $S_6, S_8, S_{10}, S_2, S_4$ must be the complement of S_1, S_3, S_5, S_7, S_9, respectively to obtain sinusoidal outputs and avoid the open- and short-circuits for the legs from b to e. Based on these constraints, Fig. 3 shows the switching states combinations of leg-a switches during the charging (S_0 is ON) and discharging processes (S_0 is OFF). It is worth noting that the discharging mode occurs only when all the upper switches are ON, i.e., at the zero-state {11111}. In this case, all the output line voltages are zero.

B. AC inversion Operating-mode

From the AC inversion point of view, to obtain the same operation of the standard VSI, the active vectors of the proposed topology must be applied during the inductive charging, i.e., S_0 is ON. In this case, the proposed topology has the same thirty active vectors, which are mapped in ten sectors as the standard five-phase VSI [23]. Fig. 4(a) shows the possible switching vectors of the proposed topology. It is important to note that the remaining zero-state {00000} is also used in charging.

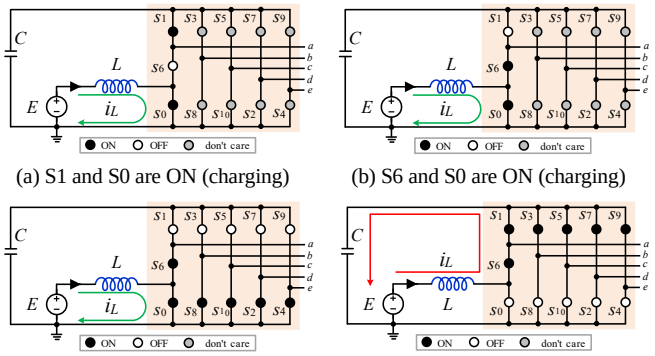

(a) S1 and S0 are ON (charging)

(b) S6 and S0 are ON (charging)

(c) S6 and the lower switches are ON (charging)

(d) S6 and the upper switches are ON (discharging)

Fig. 3. Switching actions of leg-a during inductive charging and discharging modes.

III. Proposed Vector Control Strategy

The proposed control strategy is divided into three parts. The first part is for the input-side control, the second for output-side (motor) control, and the third applies the SVPWM approach that is used to generate the switching pulses for the switches, as shown in Fig. 4.

A. Input-side control stage

The main objectives of the input-side control stage are 1) to track the reference dc-link voltage and 2) to regulate the supply current based on the power demanded and despite system disturbances or uncertainties. It consists of a cascaded dual-loop controller, as shown in Fig. 4. The reference dc-link voltage v_{dc}^* is determined from the motor ratings, while the reference current generated from the dc-voltage controller is defined by (1).

$$i_L^* = k_{p1} e_v + k_{i1} \int_0^t e_v dt \qquad (1)$$

The input current controller is dedicated to realizing a fast response of the charging duty cycle, D, where $0.1 \leq D \leq 0.9$.

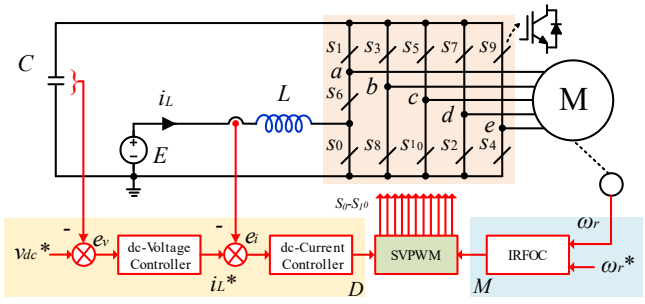

Fig. 4. Proposed control strategy for the five-phase S^{3}I topology.

B. *Output-side control stage*

The output side control part is based on the IRFOC scheme, shown in Fig. 5, which controls the output side by determining the modulation index, M and generates sinusoidal reference signals, $v_a^* - v_e^*$. It first uses the motor reference speed, ω_r^* and core reference flux, λ_{dr}^* to generate the reference torque, T_e^* and dq-current components (i_{qs}^* and i_{ds}^*) for the motor at the given conditions.

Next, the synchronous current control technique is applied to generate the reference voltages, as presented in [3] and [10]. As shown in Fig. 5, two pairs of current controllers are used to evaluate reference voltages in the synchronous reference frame. After these voltages have been converted to five-phase, they are utilized as references for modulation.

It is important to note that the machine parameters are necessary to design the IRFOC. These parameters can be practically identified using the traditional no-load and locked rotor tests [24]. In this paper, the parameters for a custom-designed five-phase machine are used.

C. *Space Vector Modulator*

Finally, the SVM modulator handles the signals from the input- and output sides' controllers to obtain the duty cycles of the active and zero vectors and generate the gating pulses.

Fig. 4 shows the available switching vectors for the first sector of space vector modeling of the proposed topology. There are six possible active vectors of the space vector dq-plane. It can be divided into large, medium, and small according to the length. In the proposed modulation scheme, the large and medium active vectors are applied in each switching cycle to obtain the boosting action and give sinusoidal output voltages. The duty cycles of these vectors are determined to cancel the xy components with minimal switching stresses. Therefore, the applied vectors in sector-1 are 1) two large (v_{24}, v_{25}), 2) two medium (v_{16}, v_{29}), and 3) three-zeros (v_0, v_{31c}, v_{31d}) as shown in Fig. 4(b), where v_{31c} is the zero vector {11111} during charging and v_{31d} is the same zero vector during the discharging process. Based on the volt-second balance concept, the reference space vector and the duty cycles of these vectors are governed by

$$\begin{cases} \vec{v}_{dq}^* = d_{16}\vec{v}_{16} + d_{24}\vec{v}_{24} + d_{25}\vec{v}_{25} + d_{29}\vec{v}_{29} + d_z\vec{v}_z \\ d_{16} + d_{24} + d_{25} + d_{29} + d_z + D = 1 \end{cases} \quad (2)$$

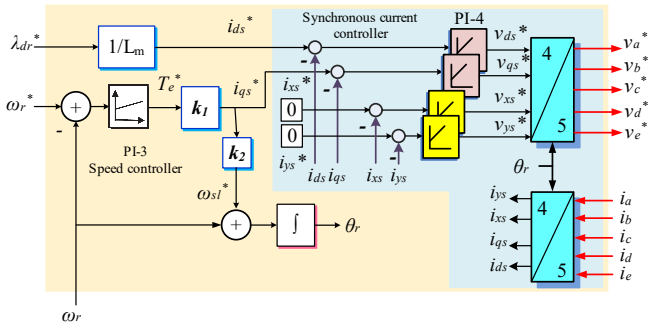

Fig. 5. Generation of the reference voltages from the IRFOC based on the SCC technique.

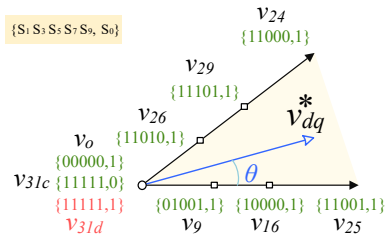

(a) Available switching vector in sector-1 of dq-subspace

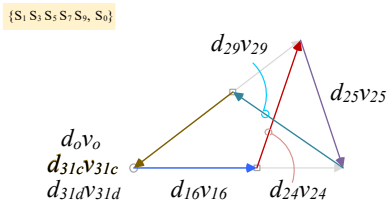

(b) Selected switching vector in sector-1 of dq-subspace

Fig. 6. Space vector representation of sector-1.

where D is the charging duty cycle.

$$\begin{cases} d_{16} = MK_1 \sin(s\pi/5 - \theta) \\ d_{24} = MK_2 \sin(\theta - (s-1)\pi/5) \\ d_{25} = MK_2 \sin(s\pi/5 - \theta) \\ d_{29} = MK_1 \sin(\theta - (s-1)\pi/5) \end{cases} \quad (3)$$

where M is the modulation index, determined from FOC, s is the sector number, K_h is a constant defined by $K_h = \sin(h\pi/5)$ and $\theta = \omega t$, while ω is the angular frequency in rad/second.

It is worth noting that the duty cycle of S_o is determined from the closed-loop controller in the drive system, which will determine this duty cycle based on the required dc-link voltage.

D. *DC-Boosting factor and Output Voltage Gain*

From the equivalent circuits of the proposed inverter during charging and discharging modes, shown in Fig. 3, the dc boosting factor, B (B is defined as the ratio between the capacitor average voltage and the supply voltage) of the proposed inverter can be calculated from

$$B = \frac{1}{1 - D} \quad (4)$$

Moreover, the voltage gain, which is defined as the ratio between the peak value of the phase voltage to the supply voltage, is

$$G = \frac{M}{2\sin(2\pi/5)\,(1 - D)} \quad (5)$$

IV. Simulation Results

Simulation models have been developed using PLECS© software for a vector control technique of a five-phase induction motor drive fed by S^{3}I. The system and motor parameters are listed in Table-I. The induction motor was simulated using $dqxy$-model in the stationary reference frame, and the dc- and ac-sides were controlled using the proposed strategy with the given parameters. The reference torque is limited to the motor-rated torque (3.75 Nm). Forced excitation is initiated before powering up the drive system to keep the rotor flux at the rated

value for speed lower than the base value. Therefore, at the time of speed reference application, the rotor flux is previously stabilized at the rated value. To verify the validity of the PLECS models developed for the proposed drive system, simulation results have been obtained for supply voltage dip, acceleration, a step change in speed, disturbance rejection, and speed reversal transients. The results shown in Figs. 7 and 8 have been classified into two case studies: 1) supply voltage dip and 2) constant supply voltage case.

TABLE I. PARAMETERS OF THE FIVE-PHASE INDUCTION MACHINE

Parameter	Value	Parameter	Value
Power [kW]	1.1	Rs [Ω]	14
Line voltage [V]	380V	Rr [Ω]	4.6
No. of poles	2-pole	Ls [H]	0.8714
Frequency [Hz]	50 Hz	Lr [H]	0.8714
Inertia	0.03	Lm [H]	0.85

TABLE II. PARAMETERS AND GAINS FOR IRFOC AND DUAL-LOOP CONTROLLER

Parameter		Value	Parameter		Value
k_1		0.695	DC voltage controller	k_p	0.5
k_2		3.042		k_i	0.04
Torque limit		3.75	DC current controller	k_p	1
Speed controller	k_p	2.67		k_i	0.5
	k_i	118.5	Initial rotor flux		1.525

A. *Supply Voltage Dip*

In this case, it is assumed that the supply voltage is 300V for the first 0.5 sec of the simulation. Afterwards, it was reduced to 250V for 0.5 sec and then restored to its original value. Moreover, the motor is accelerated at t=0.3 sec from the standstill to 1000 rpm at no-load. After that, a load of 2 Nm is applied at t=0.7 sec. The waveforms of supply voltage and the system responses are shown in Fig. 7.

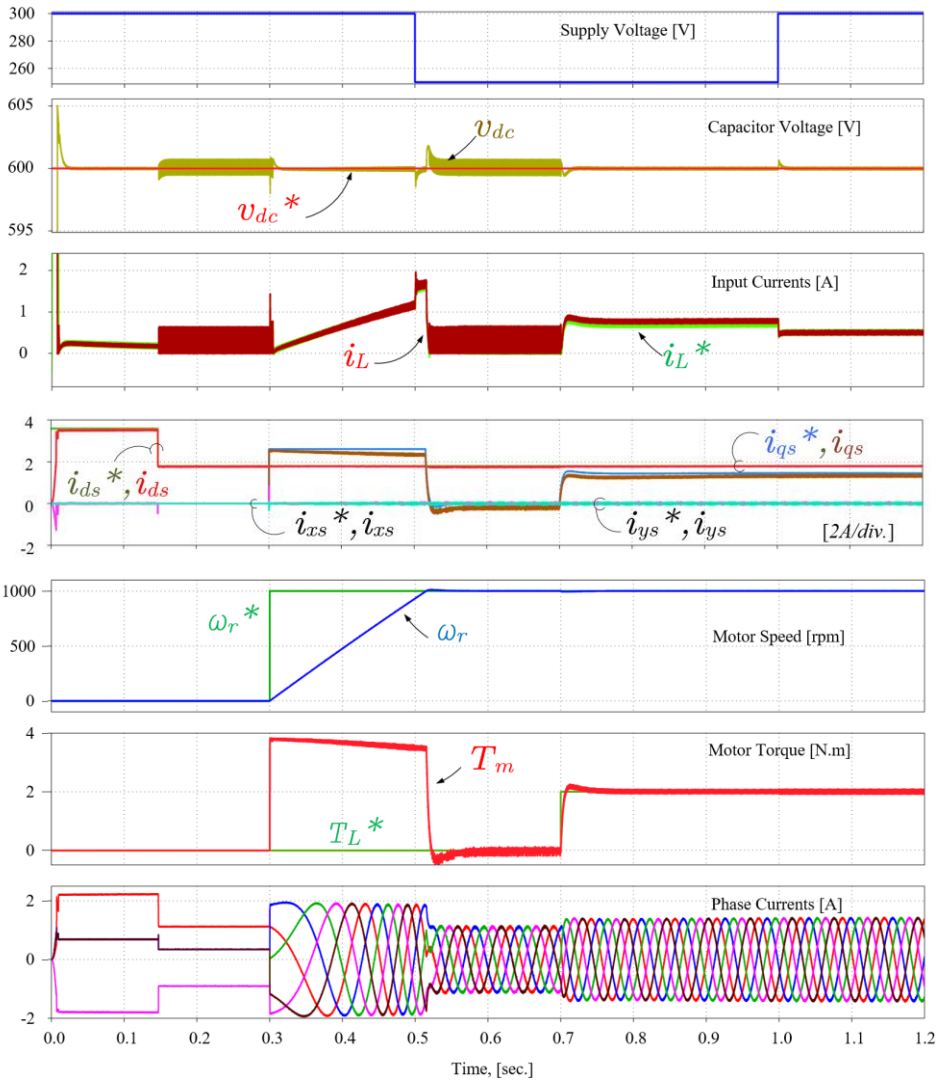

Fig. 7. Simulation results for the suggested IRFOC strategy of the proposed system for voltage dip case-study-1.

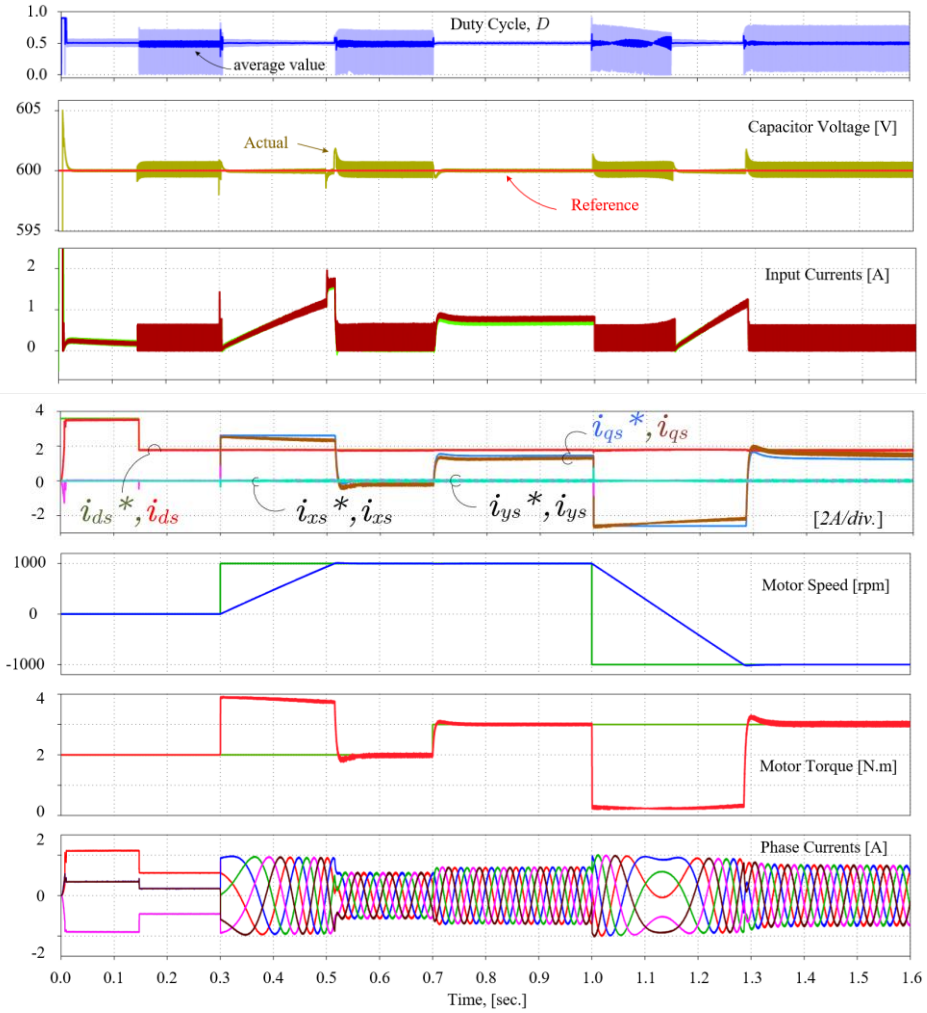

Fig. 8. Simulation results for the suggested IRFOC strategy of the proposed system for constant supply voltage (case-study-2).

As you can see from Fig. 7, the actual and reference dc-link voltage, actual and reference supply current, and speed, torque, $dqxy$ components of the motor current and actual phase currents are shown, respectively. It can be observed from that

- The proposed topology boosts the supply voltage to 600 volts at the dc-link capacitor. Furthermore, the dual loop controller is capable of following the reference dc-link voltage and the inductor current references despite disturbances with small ripples.
- The actual flux and torque components of the motor currents are fully decoupled and follow the references.
- The motor runs from the standstill to 1000 rpm in about 0.2 sec, and the motor torque follows the reference torque with a fast response.
- In addition, the motor currents have sinusoidal waveforms with a THD of less than 4.6%.

B. *Constant Supply Voltage*

In this case, the supply voltage is assumed to be a constant of 300V. An acceleration, speed step change from 0 to 1000 rpm, disturbance rejection due to applying 2Nm load at 0.7 sec and speed reversal at t=1 sec transients are examined. A sample of the obtained results is shown in Fig. 8. It can be observed that

- The dc-link voltage is boosted and regulated at its reference value, as in case 1.
- The actual torque follows the reference torque very well. In addition, the flux and torque current components are fully decoupled.
- The motor currents increase due to the loading effect at 0.7 sec but still have sinusoidal waveforms.
- The speed reversal transient is also examined at t=1 sec. The responses show that the actual motor torque closely follows the reference value, resulting in rapid speed reversal, with torque in the limit, in the shortest possible time interval (approximately 290 msec).
- The change of phase sequence in the stator current is observed because of the change in the direction.

Moreover, custom Python scripts were developed to interact with the PLECS model of the proposed topology. The scripts are used for controlling and running loop simulations and extracting results from the model that demonstrates how changing the proposed SVM scheme's modulation index can affect the proposed topology's performance. Fig. 9 shows the output

voltage's total harmonic distortion (THD) versus the modulation index. It can be observed that the THD of the output voltage is decreased when the modulation index is increased, like the VSI.

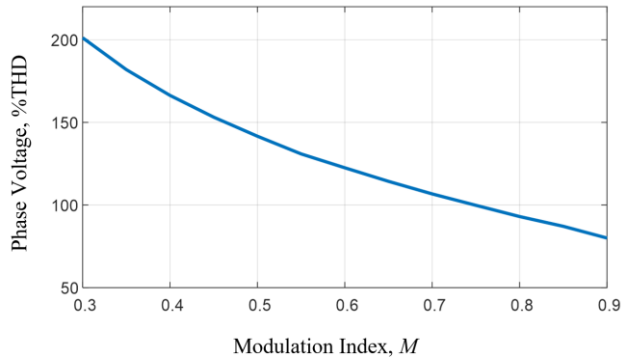

Fig. 9. Output voltage THD of the proposed S^3I using the proposed space vector modulation approach for FOC control strategy.

In summary, using the proposed control strategy, the dc-link voltage control of the proposed drive system remains constant regardless of how much the dc-supply voltage or the motor load varies. Moreover, good dynamic responses are observed from the simulation results during the case studies.

V. Conclusions

The application of a five-phase simplified split-source inverter (S^3I) for controlling an induction motor is presented. Field oriented control strategy is developed to obtain a high-performance drive system. A new space vector modulator is proposed to perform the boosting and inversion processes. The motor performances are tested using PLECS and Python. Good results during different dynamic scenarios are observed. According to the results, the proposed control algorithm presented in this paper to control the split-source inverter is advisable for industrial applications.

References

[1] M. Y. Metwly, A. S. Abdel-Khalik, M. S. Hamad, S. Ahmed and N. A. Elmalhy, "Multiphase Stator Winding: New Perspectives, Advanced Topologies, and Futuristic Applications," *IEEE Access*, vol. 10, pp. 103241-103263, 2022.

[2] S. M. Dabour, A. S. Abdel-Khalik, S. Ahmed and A. M. Massoud, "A new dual series-connected Nine-Switch Converter topology for a twelve-phase induction machine wind energy system," in Proc of CPE-POWERENG2017, Cadiz, Spain, 2017, pp. 139-144.

[3] E. Levi, "Multiphase Electric Machines for Variable-Speed Applications," *IEEE Transactions on Industrial Electronics*, vol. 55, no. 5, pp. 1893-1909, May 2008.

[4] L. Parsa and H. A. Toliyat, "Five-phase permanent-magnet motor drives," *IEEE Transactions on Industry Applications*, vol. 41, no. 1, pp. 30-37, Jan.-Feb. 2005, doi: 10.1109/TIA.2004.841021.

[5] A. S. Abdel-Khalik, A. S. Morsy, S. Ahmed and A. M. Massoud, "Effect of Stator Winding Connection on Performance of Five-Phase Induction Machines," *IEEE Transactions on Industrial Electronics*, vol. 61, no. 1, pp. 3-19, Jan. 2014, doi: 10.1109/TIE.2013.2242417.

[6] M. Bermudez, I. Gonzalez-Prieto, F. Barrero, H. Guzman, M. J. Duran and X. Kestelyn, "Open-Phase Fault-Tolerant Direct Torque Control Technique for Five-Phase Induction Motor Drives," *IEEE Trans. Ind. Electron.*, vol. 64, no. 2, pp. 902-911, Feb. 2017.

[7] S. M. Dabour, E. M. Rashad, A. Abdel-khalik, S. Ahmed and A. Massoud, "A new fifteen-switch inverter topology for two five-phase motors drive," in Proc of MEPCON2016, Cairo, Egypt, 2016, pp. 729-734.

[8] I. Jamal et al., "A Comprehensive Review of Grid-Connected PV Systems Based on Impedance Source Inverter," *IEEE Access*, vol. 10, pp. 89101-89123, 2022, doi: 10.1109/ACCESS.2022.3200681.

[9] S. M. Dabour, S. M. Allam and E. M. Rashad, "Indirect space-vector PWM technique for three to nine phase matrix converters," in Proc of 8th GCC Conference & Exhibition, Muscat, Oman, 2015, pp. 1-6.

[10] O. Ellabban and H. Abu-Rub, "Field-oriented control of a five-phase induction motor fey by a Z-source inverter," 2013 IEEE International Conference on Industrial Technology (ICIT), 2013, pp. 1624-1629, doi: 10.1109/ICIT.2013.6505916.

[11] S. Rahman, K. Rahman, M. A. Ali, M. Meraj and A. Iqbal, "Quasi Z Source Inverter Fed V/f Controlled Five-Phase Induction Motor Drive Powered," 2019 International Conference on Electrical, Electronics and Computer Engineering (UPCON), 2019, pp. 1-6, doi: 10.1109/UPCON47278.2019.8980073.

[12] R. Hammad et al., "Asymmetrical six-phase induction motor drives based on Z-source inverters: Modulation, design, fault detection and tolerance," *Alexandria Engineering J.*, Vol. 61, Issue 12, 2022.

[13] H. Ribeiro, A. Pinto and B. Borges, "Single-stage DC-AC converter for photovoltaic systems," 2010 IEEE Energy Conversion Congress and Exposition, 2010, pp. 604-610, doi: 10.1109/ECCE.2010.5617957.

[14] A. Abdelhakim, P. Mattavelli and G. Spiazzi, "Three-Phase Split-Source Inverter (SSI): Analysis and Modulation," *IEEE Transactions on Power Electronics*, vol. 31, no. 11, pp. 7451-7461, Nov. 2016.

[15] S. S. Lee and Y. E. Heng, "Improved single-phase split-source inverter with hybrid quasi-sinusoidal and constant PWM," *IEEE Trans. Ind. Electron.*, vol. 64, no. 3, pp. 2024-2031, Mar. 2017.

[16] S. S. Lee, A. S. T. Tan, D. Ishak and R. Mohd-Mokhtar, "Single-Phase Simplified Split-Source Inverter (S3I) for Boost DC–AC Power Conversion," *IEEE Transactions on Industrial Electronics*, vol. 66, no. 10, pp. 7643-7652, Oct. 2019, doi: 10.1109/TIE.2018.2886801.

[17] A. Abdelhakim, P. Mattavelli and G. Spiazzi, "Three-Phase Three-Level Flying Capacitors Split-Source Inverters: Analysis and Modulation," *IEEE Transactions on Industrial Electronics*, vol. 64, no. 6, pp. 4571-4580, June 2017, doi: 10.1109/TIE.2016.2645501.

[18] M. AbdulSalam, et al., "Cascaded Multilevel Split-Source Inverters: Analysis and Modulation," 2019 21st International Middle East Power Systems Conference (MEPCON), 2019, pp. 1204-1209, doi: 10.1109/MEPCON47431.2019.9008050.

[19] S. H. Montazeri, J. Milimonfared and M. Zolghadri, "A New Modeling and Control Scheme for Cascaded Split-Source Converter Cells," *IEEE Transactions on Industrial Electronics*, vol. 69, no. 8, pp. 7618-7628, Aug. 2022, doi: 10.1109/TIE.2021.3111559.

[20] S. M. Dabour, A. S. Abdel-Khalik, S. Ahmed and A. Massoud, "An Optimal PWM Technique for Dual-Output Nine-Switch Boost Inverters With Minimum Passive Component Count," *IEEE Transactions on Power Electronics*, vol. 36, no. 1, pp. 1065-1079, Jan. 2021, doi: 10.1109/TPEL.2020.3001372.

[21] S. M. Dabour, A. A. Aboushady, M. A. Elgenedy, I. A. Gowaid and M. E. Farrag, "Current Ripple Evaluation of Space Vector Modulated Five-Phase Split-Source Inverters," 2022 57th International Universities Power Engineering Conference (UPEC), 2022, pp. 1-6, doi: 10.1109/UPEC55022.2022.9917947.

[22] S. M. Dabour, A. A. Aboushady, I. A. Gowaid, Mohamed. A. Elgenedy, and M. E. Farrag, "Performance Analysis and Evaluation of Multiphase Split-Source Inverters," *Energies*, vol. 15, no. 22, p. 8411, Nov. 2022.

[23] S. M. Dabour, A. S. Abdel-Khalik, A. M. Massoud and S. Ahmed, "Analysis of Scalar PWM Approach With Optimal Common-Mode Voltage Reduction Technique for Five-Phase Inverters," *IEEE Journal of Emerging and Selected Topics in Power Electronics*, vol. 7, no. 3, pp. 1854-1871, Sept. 2019, doi: 10.1109/JESTPE.2018.2866028.

[24] A. S. Abdel-Khalik, M. I. Daoud, S. Ahmed, A. A. Elserougi and A. M. Massoud, "Parameter Identification of Five-Phase Induction Machines With Single Layer Windings," *IEEE Trans. Ind. Electronics*, vol. 61, no. 10, pp. 5139-5154, Oct. 2014, doi: 10.1109/TIE.2013.2297294.